Structural Engineering and Mechanics, Vol. 39, No. 5 (2011) 621-642
DOI: http://dx.doi.org/10.12989/sem.2011.39.5.621

Performance of tuned mass dampers against near-field earthquakes

E. Matta*

Structural and Geotechnical Engineering Department, Turin Politechnic, Turin, Italy

(Received July 8, 2010, Accepted May 25, 2011)

Abstract. Passive tuned mass dampers (TMDs) efficiently suppress vibrations induced by quasi-stationary dynamic inputs, such as winds, sea waves or traffic loads, but may prove of little use against pulse-like excitations, such as near-field (NF) ground motions. The extent of such impairment is however controversial, partly due to the different evaluation criteria adopted within the literature, partly to the limited number of seismic records used in most investigations. In this study, three classical techniques and two new variants for designing a TMD on an SDOF structure are tested under 338 NF records from the PEER NGA database, including 156 records with forward-directivity features. Percentile response reduction spectra are introduced to statistically assess TMD performance, and TMD robustness is verified through Monte Carlo simulations. The methodology is extended to a variety of MDOF bending-type and shear-type frames, and simulated on a case study building structure recently constructed in Central Italy. Results offer an interesting insight into the performance of TMDs against NF earthquakes, ultimately showing that, if properly designed and sufficiently massive, TMDs are effective and robust even in the face of pulse-like ground motions. The two newly proposed design techniques are shown to generally outperform the classical ones.

Keywords: structural control; tuned mass damper; near-field earthquake; PEER NGA database; robustness; optimal design

1. Introduction

Tuned mass dampers (TMDs) are well-known passive vibro-protecting devices. A TMD is basically a single-degree-of-freedom (SDOF) appendage of the primary structure (Warburton 1982). Through assigning its mass and optimizing its viscous-elastic connection to the structure, the appendage is "tuned" to the structural target mode and so made capable to "resonate" with it, absorbing part of its vibratory energy. Since the absorption mechanism requires the motion of the structure to react with, in order for the device to be effective the energy input into the system must be gradual. This is why stationary conditions are the ideal case for TMDs, which are commonly installed for wind or traffic applications on flexible low-damped structures such as tall buildings and towers, bridges and footbridges, chimneys and antennae (Wu and Cai 2009, Homma *et al.* 2009, Ubertini 2010).

On the other hand, the non-stationary nature of earthquake ground motion makes TMDs seismic

*Corresponding author, Research Scholar, E-mail: emiliano.matta@polito.it

effectiveness uncertain. In the last four decades, researchers have parted between supporters (Wirsching and Campbell 1974, Jagadish *et al.* 1979, Clark 1988, Villaverde and Koyama 1993, Bernal 1996, Jara and Aguiniga 1996, Sadek *et al*. 1997, Pinkaew *et al.* 2003, Taflanidis *et al.* 2007, Marano *et al.* 2008) and detractors (Gupta and Chandrasekaran 1969, Kaynia *et al.* 1981, Sladek and Klingner 1983, Miyama 1992, Soto-Brito and Ruiz 1999), without getting to a final verdict.

The controversy is easily explained. For a given structure, TMD seismic performance essentially depends on the ground motion features. Short-duration, impulsive records are not easily controlled through a TMD, which may be instead effective against long-duration, narrow-band ground motions. No general agreement has been found yet, essentially because every author has used one particular assembly of records, mostly very limited in number, in conjunction with one particular choice of design method, performance measures and structural schematization. In fact, most studies consider only one record, e.g., Mexico City (Villaverde and Koyama 1993, Bernal 1996, Jara and Aguiniga 1996, Pinkaew *et al.* 2003), Taft (Gupta and Chandrasekaran 1969, Jagadish *et al.* 1979), El Centro (Sladek and Klingner 1983, Lin *et al*. 2001); or two records, e.g., Mexico City and Loma Prieta (Villaverde and Koyama 1993), Mexico City and El Centro (Rana and Soong 1998), Mexico City from two distinct events (Soto-Brito and Ruiz 1999), Mexico City and Bangkok (Lukkunaprasit and Wanitkorkul 2001), El Centro and Imperial Valley (Park and Reed 2001), El Centro and Kern Country (Abdullah *et al.* 2001), Kobe and Chi-Chi (Wang and Lin 2005), Kobe and Northridge (Wong 2008); or anyway very few records, e.g., 3 (Villaverde 1985), 4 (Tsai 1995), 5 (Lin *et al.* 1999). Only few studies use a representative number of records, e.g., 12 (Taniguchi *et al*. 2008), 13 (Chen and Wu 2001), 18 (Pourzeynali and Zarif 2008), 48 (Kaynia *et al.* 1981), 52 (Sadek *et al.* 1997). Other studies simulate ground motion through analytical signals, e.g., harmonic (Abe 1996), harmonic of finite duration (Tsai 1995), white-noise scaled by time-modulating functions (Sinha and Igusa 1995); or as stochastic processes, e.g., white noise (Wirsching and Campbell 1974), Kanai-Tajimi coloured noise (Chen and Wu 2001, Hoang *et al.* 2008), evolutionary process (Jangid 2004, Leung *et al.* 2008).

In an effort to solve the said controversy, this paper statistically quantifies TMDs seismic performance using the largest set of historical records ever reported for TMD evaluation. In the spirit of a worst-case assessment, the selected set entirely consists of near-field (NF) earthquakes, known to be critical for TMDs applications because of their potential impulsive features (Lukkunaprasit and Wanitkorkul 2001, Taniguchi *et al.* 2008, Pourzeynali and Zarif 2008). In fact, NF shaking can be characterized by a short-duration impulsive motion that exposes structures to high input energy at the beginning of the record (Bray and Rodriguez-Marek 2004). This pulse-type motion, particular to the "forward" direction and therefore denoted as "forward-directivity" (FD) effect (Somerville *et al.* 1997), occurs when the fault rupture propagates towards the site at a velocity close to the shear wave velocity, causing most of the seismic energy to arrive at the site within a short time, in the form of a large energy pulse at the beginning of the record. Under this type of ground motion, there is little time for transferring energy from the primary structure into a TMD. Although such control impairment is generally acknowledged (Taniguchi *et al.* 2008, Pourzeynali and Zarif 2008), no statistically consistent quantification of its extent is presently reported in the literature.

In this paper, 338 NF records from the PEER NGA strong motion database, including 156 records with FD features, are used to test a TMD on a variety of SDOF and multi-degrees-of-freedom (MDOF) structures. Analysis is restricted to linear structural systems for the sake of simplicity. Five

different design methods are compared, including three classical techniques and two original ones. Percentile response reduction spectra are introduced to statistically assess TMD performance, and TMD robustness is verified through Monte Carlo simulations. Large mass ratios are assumed for the TMD at the design stage as a precondition for a satisfactory seismic performance. Namely, the "effective mass ratio" is taken to be as high as 10% or 50%, roughly corresponding, for an MDOF bending-type structure (see Section 4 next), to a TMD mass equalling, respectively, 3% or 15% the total mass of the building. Though considerably larger than usual, these mass ratios are not at all impractical, and can be operatively achieved, for instance, by recurring to concepts such as the "expendable top storey" (Jagadish *et al.* 1979), the "energy absorbing storey" (Miyama 1992), the "additional isolated upper floor" (Melkumyan 1996), the "mega-substructure configuration" (Sadek *et al.* 1997), or the more recent "roof-garden TMD" (RGTMD) proposed by the author in (Matta and De Stefano 2009). The simulation of a RGTMD on a building structure recently constructed in Central Italy is finally presented in order to demonstrate the feasibility of the proposed design methodology and the satisfactory performance of a properly designed TMD against NF ground motions.

2. The ensemble of earthquake records

The whole of NF records used for analysis comes from the PEER NGA strong-motion database, currently consisting of 3551 publicly available multi-component records of 173 shallow crustal earthquakes from active tectonic regions world wide (Chiou *et al.* 2008).

Records from the PEER NGA database are here collected through assembling sets identified in previous studies as representative of strong NF ground motions and/or pulse-like records. Three suites of two-components records are borrowed from the literature:

Suite 1: 70 pulse-like NF ground-motion pairs derived by Tothong and Cornell (2007) and subsequently used, e.g., also in (Baker and Cornell 2008) as «a collection of the pulse motions identified by Mavroeidis and Papageorgiou (2003), Fu and Menun (2004), and Bazzurro and Luco (2004)», in which the occurrence of at least one pulse was ascertained by visual inspection. The earthquake moment magnitude, M_w, ranges from 5.6 to 7.6, and the station-to-rupture distance, R, from 0.07 to 22 km.

Suite 2: 52 pulse-like NF ground-motion pairs used by Bray and Rodriguez-Marek (2004) as representative of FD ground motion (based on Somerville criterion of fault-normal to fault-parallel spectral ratio), characterized by $M_w > 6$. Stations at $R \leq 20$ km for earthquakes with $M_w \geq 6.5$ and $R \leq 15$ km for $M_w < 6.5$, and a spectral ratio at 3s greater than one are considered.

Suite 3: 147 strong NF (with and w/o FD features) ground-motion pairs used by Huang *et al.* (2008), including earthquakes with $M_w \geq 6.5$ and $R \leq 15$ km.

Suites 1 to 3 are then assembled in the following two sets:

- FD set (merging Suite 1 and Suite 2): 78 ground-motion pairs (156 accelerograms) representative of NF earthquakes with forward directivity.
- NF set (merging Suite 1, Suite 2 and Suite 3): 169 ground-motion pairs (338 accelerograms) representative of NF earthquakes with or w/o forward directivity.

Earthquakes included in the NF set are listed in Table 1, together with the correspondent number of pairs occurrences. Although most seismic codes define the NF zone as being within 15 km of an active fault, station-to-rupture distances up to 22 km and 20 km are respectively included in Suites

Table 1 Earthquakes included in the NF set

Occurrences	Earthquake Name	Year	M_W	Occurrences	Earthquake Name	Year	M_W
1	Imperial Valley, USA	1940	6.95	4	Whittier Narrows, USA	1987	5.99
2	Parkfield, USA	1966	6.10	13	Loma Prieta, USA	1989	6.93
1	San Fernando, USA	1971	6.61	1	Sierra Madre, USA	1991	5.61
1	Gazli, USSR	1976	6.80	1	Erzincan, Turkey	1992	6.69
1	Tabas, Iran	1978	7.35	3	Cape Mendocino, USA	1992	7.01
21	Imperial Valley, USA	1979	6.53	2	Landers, USA	1992	7.28
1	Coyote Lake, USA	1979	5.74	21	Northridge, USA	1994	6.69
3	Irpinia, Italy	1980	6.90	5	Kobe, Japan	1995	6.90
1	Coalinga, USA	1983	6.36	6	Kocaeli, Turkey	1999	7.51
4	Morgan hill, USA	1984	6.20	56	Chi-Chi, Taiwan	1999	7.62
3	Nahanni, Canada	1985	6.76	8	Düzce, Turkey	1999	7.14
3	N. Palm Springs, USA	1986	6.06	1	Hector Mine, USA	1999	7.13
5	Superstition Hills, USA	1987	6.54	1	Denali, Alaska	2002	7.90

1 and 2, to broaden the number of useable records. Records downloaded from the PEER NGA database are here used with no further correction, i.e., neither rotation nor amplitude scaling. Avoiding amplitude scaling provides an ensemble of records whose amplitude distribution is, grossly speaking, statistically representative of the seismic hazard for a building located in a generic NF zone.

3. The performance of a TMD on an SDOF structure

3.1 TMD optimal design

Let us denote as m_s, ω_s and ζ_s, respectively, the mass, the circular frequency and the damping ratio of the SDOF structure, and as m_t, ω_t and ζ_t the corresponding parameters of the TMD. Let us define as $\mu = m_T/m_S$ the mass ratio, and as $r = \omega_t/\omega_s$ the frequency ratio of the TMD. In general, any design methodology will consist in: (i) arbitrarily fixing the value of the mass ratio μ (based on costs/benefits considerations), and (ii) accordingly finding the TMD parameters r and ζ_t which make the 2-DOF combined system (obtained mounting the TMD on the structure) optimal with respect to some desired objective. Depending on the chosen objective, various analytical or numerical optimization criteria are available.

The most widespread criteria aim at minimizing a given norm of some input-output transfer functions (TF) of the 2-DOF combined system. The TF from the ground acceleration to the structural displacement relative to the ground, here denoted as T_{du}, is typically preferred. Depending on the chosen norm, such criteria can be mainly distinguished into the H_2-norm design (Wirsching and Campbell 1974, Lin *et al.* 1999, Wang and Lin 2005, Hoang *et al.* 2008) and the H_∞-norm design (Sladek and Klingner 1983, Tsai 1995, Rana and Soong 1998, Park and Reed 2001, Pinkaew *et al.* 2003, Li and Qu 2006, Matta and De Stefano 2009).

An alternative criterion, which found limited diffusion and arose some criticism (Tsai 1995, Hoang *et al.* 2008), aims instead at maximizing damping in the two complex modes of the

combined system, as suggested by Villaverde *et al.* (1993) and Sadek *et al.* (1997).

A further criterion, recently explored by very few authors and not yet a standard approach, aims at minimizing the average response of the combined system to a set of assigned time-histories (Pourzeynali and Zarif 2008).

In the present study, five optimization criteria are compared, defined as follows:

- H_2 (minimization of the H_2-norm of T_{du}), with the optimal parameters expressed (Hoang *et al.* 2008) by

$$r = \frac{\sqrt{1-\mu/2}}{1+\mu} - \frac{0.7\varsigma_s}{1-\mu/2} \quad \text{and} \quad \varsigma_t = \sqrt{\frac{\mu(1-\mu/4)}{4(1+\mu)(1-\mu/2)}} + 0.25\mu\varsigma_s \tag{1}$$

- H_∞ (minimization of the H_∞-norm of T_{du}), with the optimal parameters numerically derivable as explained in Matta and De Stefano (2009);
- $D_{\max}$ (maximization of modal damping), with the optimal parameters expressed (Sadek *et al.* 1997) by

$$r = \frac{1}{1+\mu}\left(1 - \varsigma_s\sqrt{\frac{\mu}{1+\mu}}\right) \quad \text{and} \quad \varsigma_t = \frac{\varsigma_s}{1+\mu} + \sqrt{\frac{\mu}{1+\mu}} \tag{2}$$

- H_2^f (minimization of the H_2-norm of T_{du} multiplied by a Kanai-Tajimi filter whose circular frequency ω_g equals the structural frequency ω_s and whose damping ratio ζ_g is set to 0.3), with the optimal parameters expressed (Hoang *et al.* 2008) by

$$r = \frac{\sqrt{(1-0.6\mu)(1+\mu^2)}}{1+\mu} - 0.7\varsigma_s \quad \text{and} \quad \varsigma_t = \sqrt{\frac{\mu(1+2.5\mu+2\mu^2)}{2(1+2.7\mu)}} \tag{3}$$

- H_∞^f (minimization of the H_∞-norm of T_{du} multiplied by a Kanai-Tajimi filter having $\omega_g = \omega_s$ and $\zeta_g = 0.3$), with the optimal parameters numerically derivable similarly as for the abovementioned H_∞ method.

While H_2, H_∞ and $D_{\max}$ are well-known traditional methods, H_2^f and H_∞^f are original contributions of the present paper, although certainly related to the filtered H_2 and H_∞ design methods commonly used in automatic control, and particularly inspired to an improved version of the H_2 design recently proposed by Hoang *et al.* (2008), in which the input-output TF is multiplied, prior to minimization, by a Kanai-Tajimi filter, in order to incorporate specific site-related seismological information. In classical filtered control theory, however, and in Hoang's formulation as well, filtering presumes the prediction of the ground motion spectrum (namely, the knowledge of the ω_g/ω_s ratio), and implies that the TMD shall be optimum with respect to that particular spectrum. In the H_2^f and the H_∞^f methods proposed in this study, instead, no *a priori* information is supposed available on the earthquake spectrum at the design stage, so the input filter assumes a new meaning: systematically centred on the structural frequency ($\omega_g = \omega_s$), it no longer describes the most likely excitation but statistically enhances the performance (and robustness) of the TMD by optimizing it for the worst possible scenario, in fact corresponding to the case in which the structure is "tuned" to the earthquake, i.e., $\omega_g = \omega_s$. Not requiring a prediction of the input features, the new H_2^f and H_∞^f methods are thus as simple and "inexpensive" as the $D_{\max}$ method and as their non-filtered counterparts, H_2 and H_∞. In the sequel, the five said methods will be applied, for the sake of comparison, to the design of a TMD having a mass ratio μ equal to alternatively 10% or 50%, placed on an SDOF linear structure having damping ratio $\zeta_s = 2\%$. The optimum TMD parameters obtained with the five methods are reported in Table 2.

Table 2 Optimum TMD parameters according to the five design criteria

μ	Parameters	H_2	H_∞	$D_{\max}$	H_2^f	H_∞^f
10%	r	0.871	0.873	0.904	0.872	0.871
	ζ_t	0.153	0.194	0.320	0.140	0.187
50%	r	0.559	0.556	0.659	0.610	0.612
	ζ_t	0.314	0.408	0.591	0.249	0.322

3.2 TMD performance evaluation

In this paper, TMD performance is measured by proper *reduction ratios*, obtained dividing the uncontrolled response by the controlled response. For an SDOF structure, three response quantities are considered: the peak of the structural relative (to the ground) displacement, denoted as d; the root-mean-square (RMS) of the structural relative velocity, denoted as v; the peak of the structural absolute acceleration, denoted as A. Accordingly, the three reduction ratios, denoted as d_R, v_R, and A_R, reflect the TMD capacity to mitigate, respectively, the maximum internal forces, the low-cycle fatigue accumulated damage, and the inertial forces on non-structural elements. Since TMD performance depends on the ground motion features as well as on the structural dynamic properties, multiple structures and multiple records are to be considered.

Multiplicity of structures is achieved by varying the structural period $T = 2\pi/\omega_s$ from 0 to 10s (while keeping at 2% the structural damping ratio), and accordingly evaluating the uncontrolled and controlled response spectra, in terms of d, v, and A. Large values of T are included so as to catch the long-period impulses typical of FD ground motions. For example, using an H_2^f-optimal TMD with $\mu = 50\%$ and referring to the Northridge 1084 SCS142 record, Fig. 1 shows the time-history of the ground acceleration $u(t)$ (on the left) and the corresponding uncontrolled and controlled displacement spectra d (on the right). The effect of the absorber is clearly to "smooth" the peaks occurring in the uncontrolled spectrum whenever the structural frequency is "tuned" to significant ground motion frequency components. In the author's opinion, this peculiarity of TMDs makes the

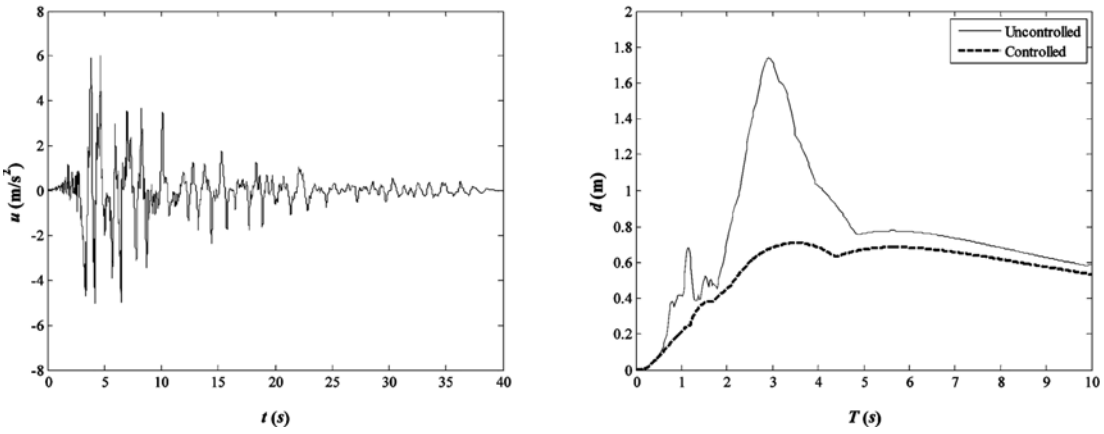

Fig. 1 Record # 1084 SCS052: (left) input accelerogram, (right) uncontrolled and controlled displacement spectra, for an H_2^f-designed TMD having $\mu = 50\%$

spectral representation an indispensable measure of TMD seismic performance. Part of the existing controversy on TMDs seismic efficacy comes from many conclusions having been drawn considering single structural periods instead of entire spectra.

Multiplicity of records, on the other hand, is achieved by repeating the spectral evaluation for the whole of ground motions included in, respectively, the FD set and the NF sets.

Then the fundamental question arises as to how to "arbitrarily" condense that multitude of structures and records into some concise index of TMD performance. Considering only the maximum reduction ratio (e.g., d_R = 2.8 at T = 1.15s in Fig. 1) would overemphasize the advantages of the device, whilst averaging over the entire range of periods would underestimate it (overlooking the merit to intervene when the structure is more exposed). The same consideration holds if, fixing a specific value of T, several spectra are observed: the maximum ratio would be an unfair choice, the average ratio a too prudential one.

So, the following statistical processing is proposed. For each T, uncontrolled and controlled spectral ordinates are first computed for the whole set of records and therefore separately sorted in ascending order, thus resulting in two "probability distribution functions"; then, dividing point-by-point the uncontrolled distribution to the controlled one, the "reduction distribution" is obtained for that T. Repeating the procedure for the entire range of periods, a spectrum of reduction distributions is obtained, which can be equivalently intended as a distribution of "reduction spectra", whence any desired percentile spectrum can be extracted. Finally, averaging along the T axis provides the average reduction distribution, from here on called the "performance curve", whence any desired percentile can be extracted.

To clarify these concepts, still referring to an H_2^f-optimal TMD with μ = 50%, and considering for example the NF set and the structural period T = 5s, Fig. 2 reports (on the left) the uncontrolled and controlled probability distribution functions of the peak relative displacement d. On the right, the corresponding "reduction distribution" d_R is reported. Rigorously speaking, the latter is not a probability distribution function, contrary to the curves on the left. In fact, according to the curves on the left, there is 95% probability that the controlled (respectively uncontrolled) displacement be 0.86(respectively 1.44)m, i.e., the controlled (uncontrolled) 95% percentile is ≤0.86(1.44)m.

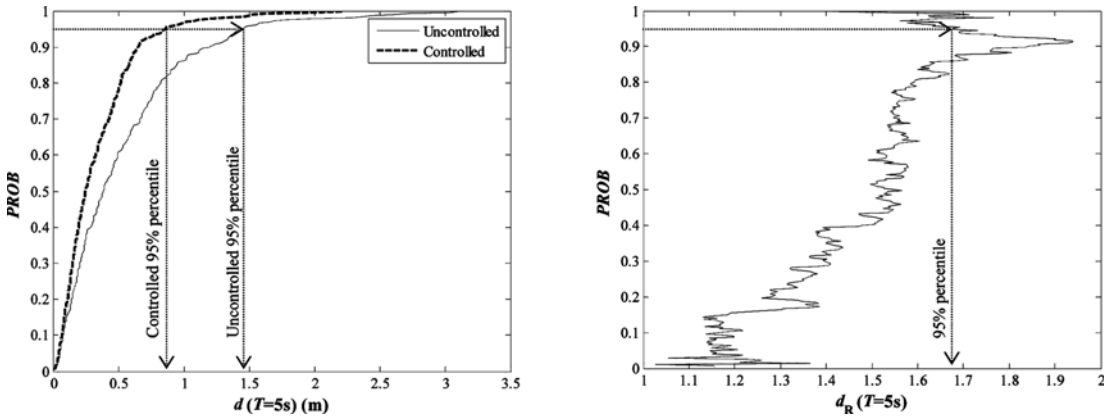

Fig. 2 Effects of an H_2^f-designed TMD with μ = 50% on a structure having T = 5s under the NF set: uncontrolled and controlled displacement probability distribution functions (left), displacement reduction distribution (right)

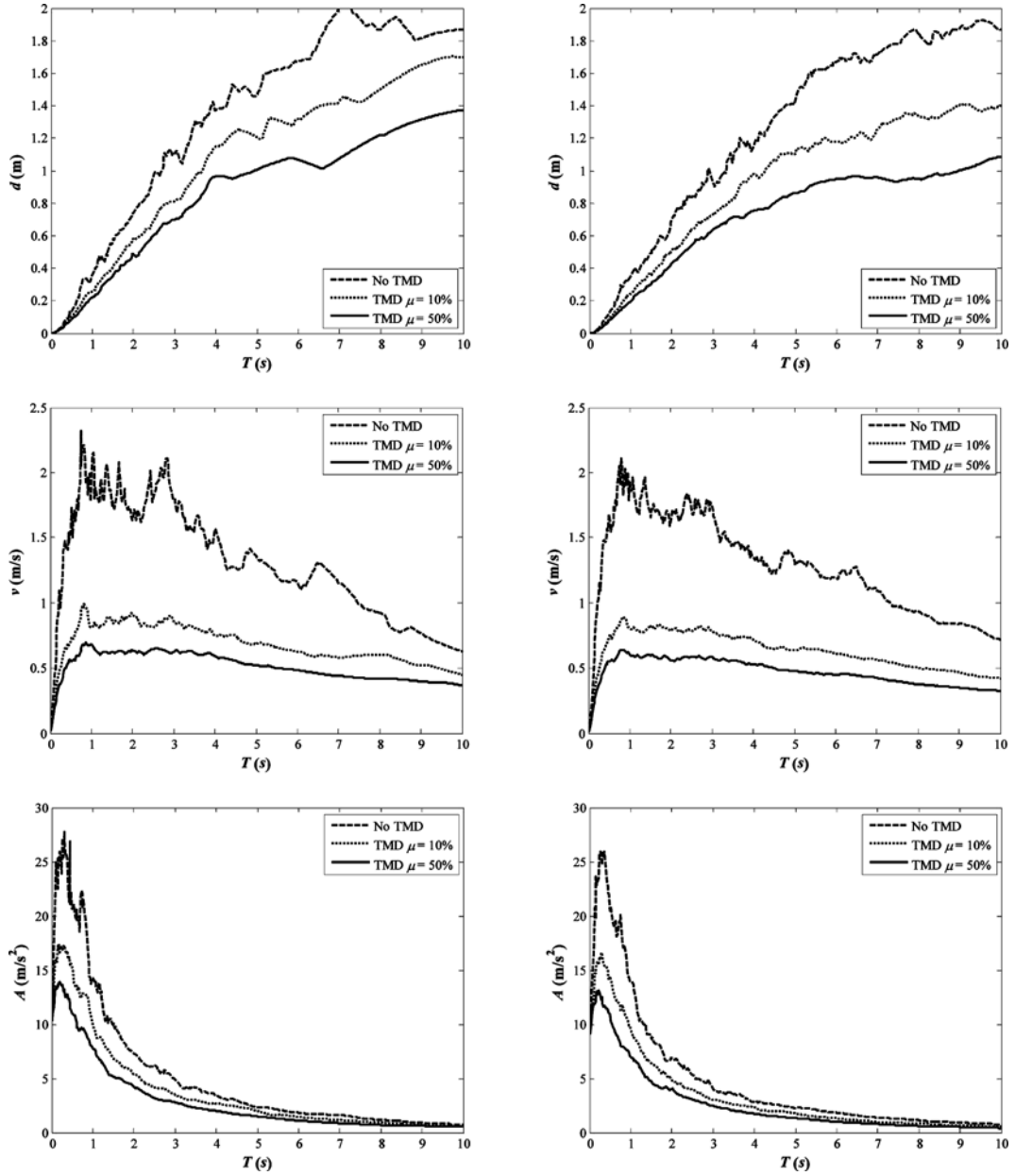

Fig. 3 95% percentile response spectra with and w/o an H_2^f-designed TMD having alternatively μ = 10% or μ = 50%: (left) FD set; (right) NF set

According to the curve on the right, the uncontrolled 95% percentile is 1.44/0.86 = 1.68 times the controlled 95% percentile, and only in this sense the 95% percentile performance is 1.68. With this in mind, the label "PROB" will be maintained for the ordinate axis, for simplicity.

Repeating the procedure above for any T in the 0-10s range, the distributions of uncontrolled and controlled response spectra are obtained. From such distribution, the 95% percentile (a reference

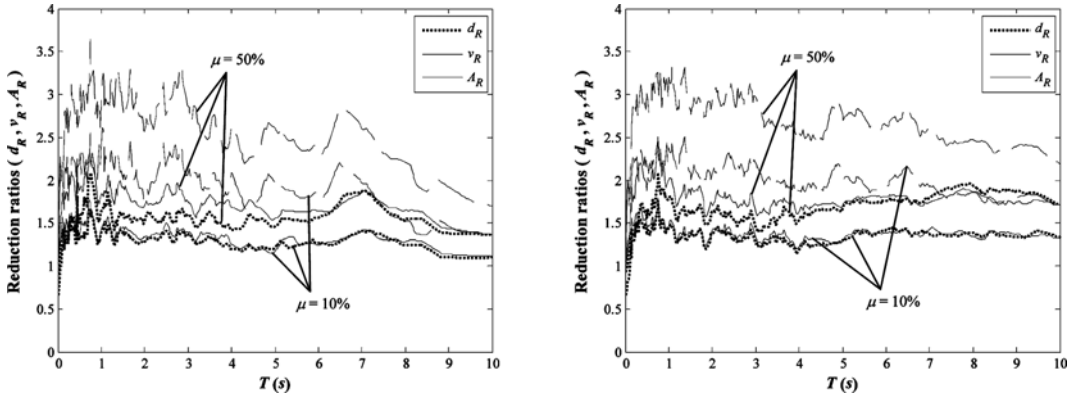

Fig. 4 95% percentile reduction spectra for an H_2^f-designed TMD having alternatively μ = 10% or μ = 50%: (left) FD set, (right) NF set

value for design loads at ultimate limit states in many building codes) is extracted and plotted in Fig. 3. The corresponding reduction spectra are plotted in Fig. 4.

Finally, repeating the analysis for every percentile and for each optimization criterion, and averaging the reduction spectra along the T axis, the performance curves for d_R, v_R and A_R are obtained as shown in Fig. 5, respectively for the FD set (on the left) and for the NF set (on the right).

Looking at Figs. 3 to 5 the following observations can be made.

- TMDs are robust with respect to the ground motion frequency content, i.e., they prove effective when more needed and nearly ineffective when less required. The spectral peak "smoothing" effect observed in Fig. 1 is confirmed in Fig. 3, as a result of TMDs being maximally effective when structure-to-earthquake "tuning" is maximum. Thus, averaging along T the reduction spectra in Fig. 4 makes the performance curves in Fig. 5 a conservative measure of TMD performance. The inclination of these curves clearly proclaims TMDs intrinsic robustness against the severity of seismic effects: no matter which design strategy is adopted, response reduction increases with the increase in the response percentile. Looking exclusively at the mean spectrum (approximated by the 50% percentile) wouldn't offer a real understanding of TMD seismic benefits, systematically underestimating it.
- TMDs are useless (maybe even detrimental) as $T \rightarrow 0$s, and their effectiveness is nearly constant elsewhere. A "rigid" structure, feeling the earthquake as a quasi-static excitation, accelerates like the ground with no significant dynamic amplification, so that the TMD acts as an inertial mass, proportionally increasing structural displacements while unchanging structural accelerations. This result is not new: averaging response spectra from 26 ground motion pairs, Sadek *et al.* (1997) concluded that, for «structures with periods 0.1-0.2s, TMDs are not effective». Here, however, the phenomenon appears more circumscribed, and that conclusion must be relaxed. First of all, it regards only d_R, and not v_R or A_R. Secondarily, the structural period below which TMDs result ineffective drops to about 0.05s for μ = 10% and to about 0.10s for μ = 50%. Above these periods, TMDs effectiveness is nearly constant with T.
- TMD effectiveness depends on the observed output measures. As expected, the RMS velocity is by far the response which benefits the most from the absorber. This indicates that a significant reduction of the low-cycle fatigue accumulated damage is generally obtained even in the case of

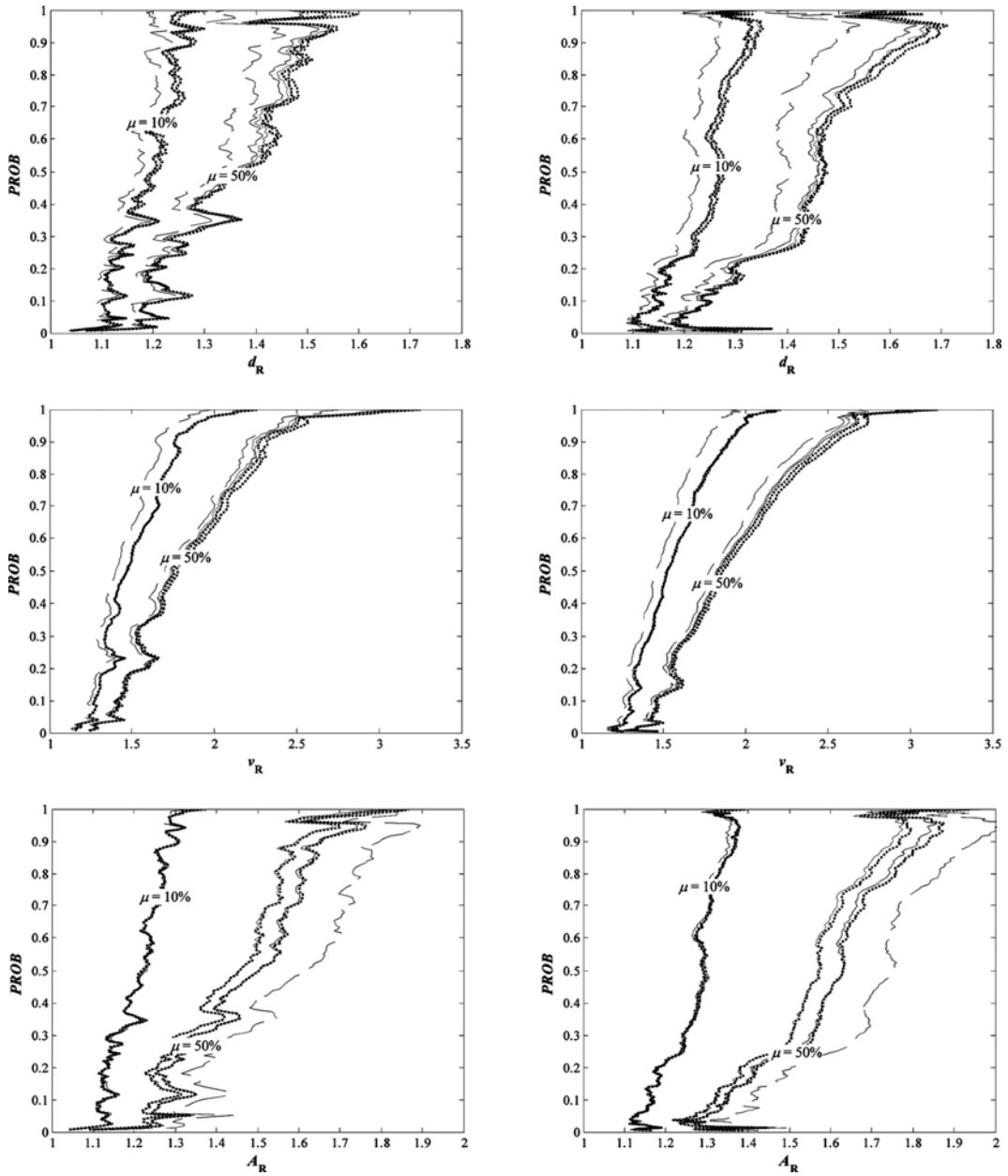

Fig. 5 Displacement, velocity and acceleration performance curves for $\mu = 10\%$ and $\mu = 50\%$, using different design methods (—— H_2; —— H_∞; - - - - D_{max}; - - - - H_2^f; - - - - H_∞^f): (left) FD set, (right) NF set

limited peak response mitigation. Less intuitively, the peak acceleration results more effectively controlled than the peak displacement.

- TMD effectiveness depends on the applied design method. The new filtered techniques are systematically superior to their classical counterparts. D_{max} is normally the less effective method, except in terms of acceleration reduction, where it appears equivalent to the others methods for

μ = 10% and by far the best for μ = 50%. Since no *a priori* information on the earthquake frequency content is needed to apply the filtered methods, their adoption is strongly recommended. In both the filtered and non-filtered variants, a trade-off appears between the H_2 and H_∞ strategies, with the former generally preferable for reducing d, the latter for reducing v and A.

- TMD effectiveness depends on the pulse-like character of the input. Focusing, for simplicity, on the 90-95% range of percentiles and on the H_2^f design, the adoption of $\mu = 10\%$ provides reductions which, for respectively the FD (and NF) sets, take on the following values: $d_R = 1.30(1.35)$, $v_R = 1.88(1.99)$, $A_R = 1.32(1.38)$; while the adoption of $\mu = 50\%$ provides: $d_R = 1.56(1.71)$, $v_R = 2.49(2.66)$, $A_R = 1.69(1.80)$. Thus, on geometrical average, the TMD performance increases 1.05 times when passing from the FD to the NF set for $\mu = 10\%$, and 1.08 times for $\mu = 50\%$. Notably enough, A_R improves to 1.90(2.02) for $\mu = 50\%$ if the $D_{\max}$ method is used. Generalizing, TMD effectiveness on linear SDOF structures is only slightly worsened by the impulsive character of FD records, and satisfactory in absolute terms, provided that large mass ratios are adopted.
- TMD effectiveness increases with the mass ratio. When passing from μ = 10% to μ = 50%, TMD performance increases, on geometrical average, 1.23, 1.33 and 1.29 times for, respectively, d_R, v_R and A_R. Improvement is less than proportional to the mass ratio increment, but far from negligible. This cost/benefit trade-off must be carefully considered when selecting the amount of mass at the design stage.

4. The performance of a TMD on an MDOF structure

A single TMD on an MDOF planar structure can not control but a single target mode (typically the fundamental one) and may therefore prove inadequate if the earthquake induces multiple-mode responses, as is typical for tall buildings (Clark 1988), especially if acceleration reduction is desired (Chen and Wu 2001).

Six distinct models are here considered of an MDOF structure, each representing a 10-storey building having constant inter-storey height and constant mass for each storey, with the TMD atop tuned to the fundamental mode. The number of storeys is large enough to satisfactorily approximate a continuous-mass cantilever beam. The first three models (S_1, S_2, S_3) reproduce a shear-type scheme, the other three (B_1, B_2, B_3) a bending-type scheme. S_1 and B_1 have constant inter-storey stiffness along the height of the structure; S_2 and B_2 have a linearly decreasing sectional stiffness with base-to-top stiffness ratio equal to 4; S_3 and B_3 have a linearly decreasing sectional stiffness with base-to-top stiffness ratio equal to 16. Damping equals 2% in each mode. Response spectra are computed by varying the fundamental period T in the range 0-10s.

Again, μ = 10% and μ = 50% are considered. Yet, according to the SDOF/MDOF equivalence established by Warburton (1982), the mass ratio μ (termed the "effective mass ratio" in distinction from the "total mass ratio") is here defined as the ratio of the absorber mass, m_t, to the effective modal mass of the target mode, m_{1eff}, on its turn defined as the target modal mass, m_1, divided by the amplitude, ϕ_{1top}, of the mass-normalized target modeshape at the TMD position. As a result, μ can be much larger than the "total mass ratio" μ_{tot}, defined as the ratio of the absorber mass to the total structural mass M. In Table 3 the main dynamic parameters are reported for the six models (f_i and m_i being the frequency and the modal mass of the i-th mode). Considering for instance the B_1

Table 3 Main dynamic parameters of the six MDOF models used in simulations

Parameters	S_1	S_2	S_3	B_1	B_2	B_3
f_2 / f_1	2.98	2.57	2.13	6.30	5.46	4.99
f_3 / f_1	4.89	4.14	3.38	17.7	14.6	12.5
m_1 / M	0.848	0.775	0.695	0.645	0.622	0.610
m_2 / M	0.091	0.122	0.145	0.198	0.194	0.187
m_3 / M	0.031	0.044	0.067	0.068	0.074	0.076
μ_{tot} / μ	0.528	0.406	0.279	0.300	0.283	0.273

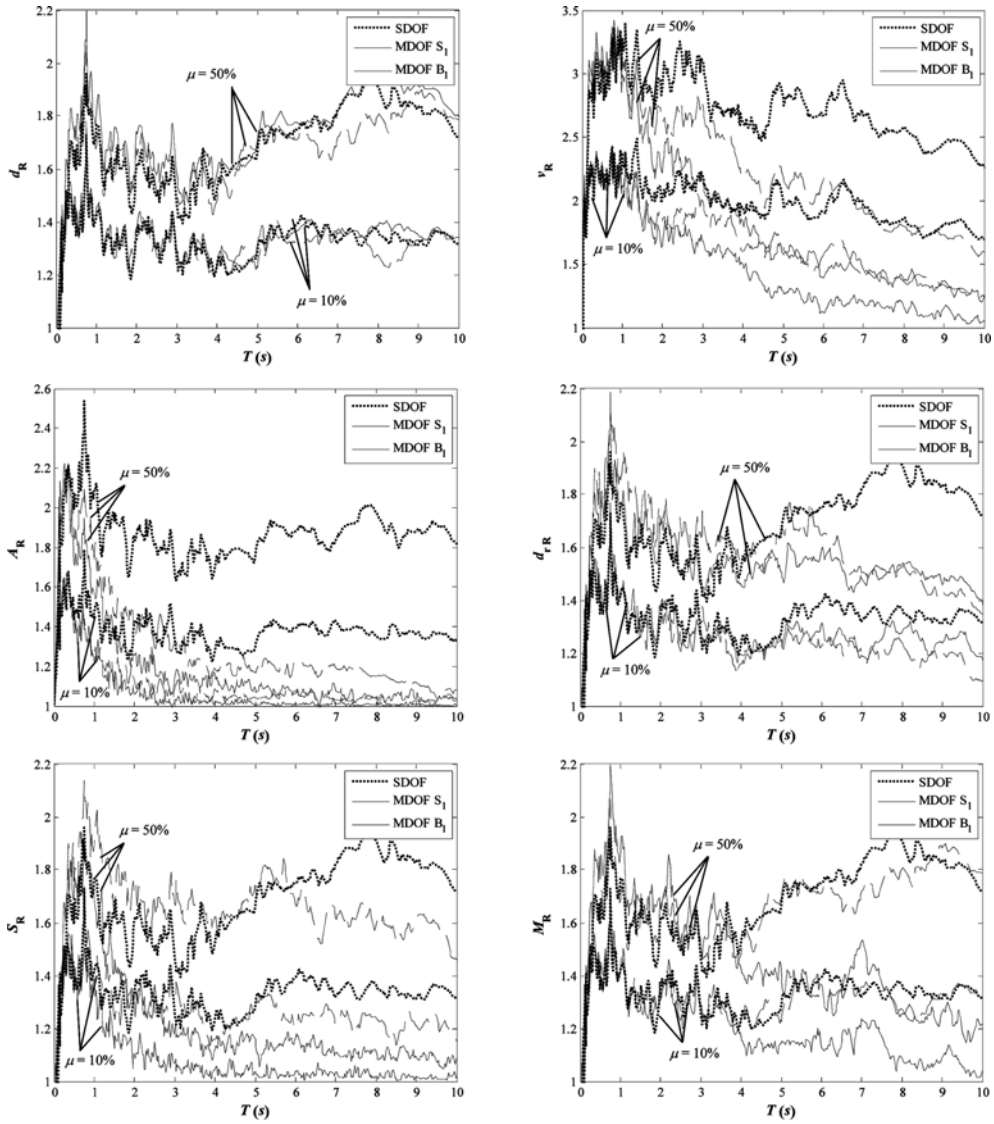

Fig. 6 95% percentile reduction spectra for an H_∞^f-designed TMD on alternatively the SDOF, the S_1 and the B_1 systems subjected to the NF set ($\mu = 10\%$ or $\mu = 50\%$)

model (μ_{tot}/μ = 0.3), the desired μ = 10% is obtained using a TMD mass which is only 0.3·10% = 3% the total mass of the building. In other words, a 3% total mass ratio is expected, according to Warburton's principle, to be as effective for the MDOF B_1 structure as the 10% is for the SDOF structure, as far as the higher modes contribution is negligible. This indicates that the large 10% and 50% effective mass ratios assumed in the present study are indeed a practicable solution.

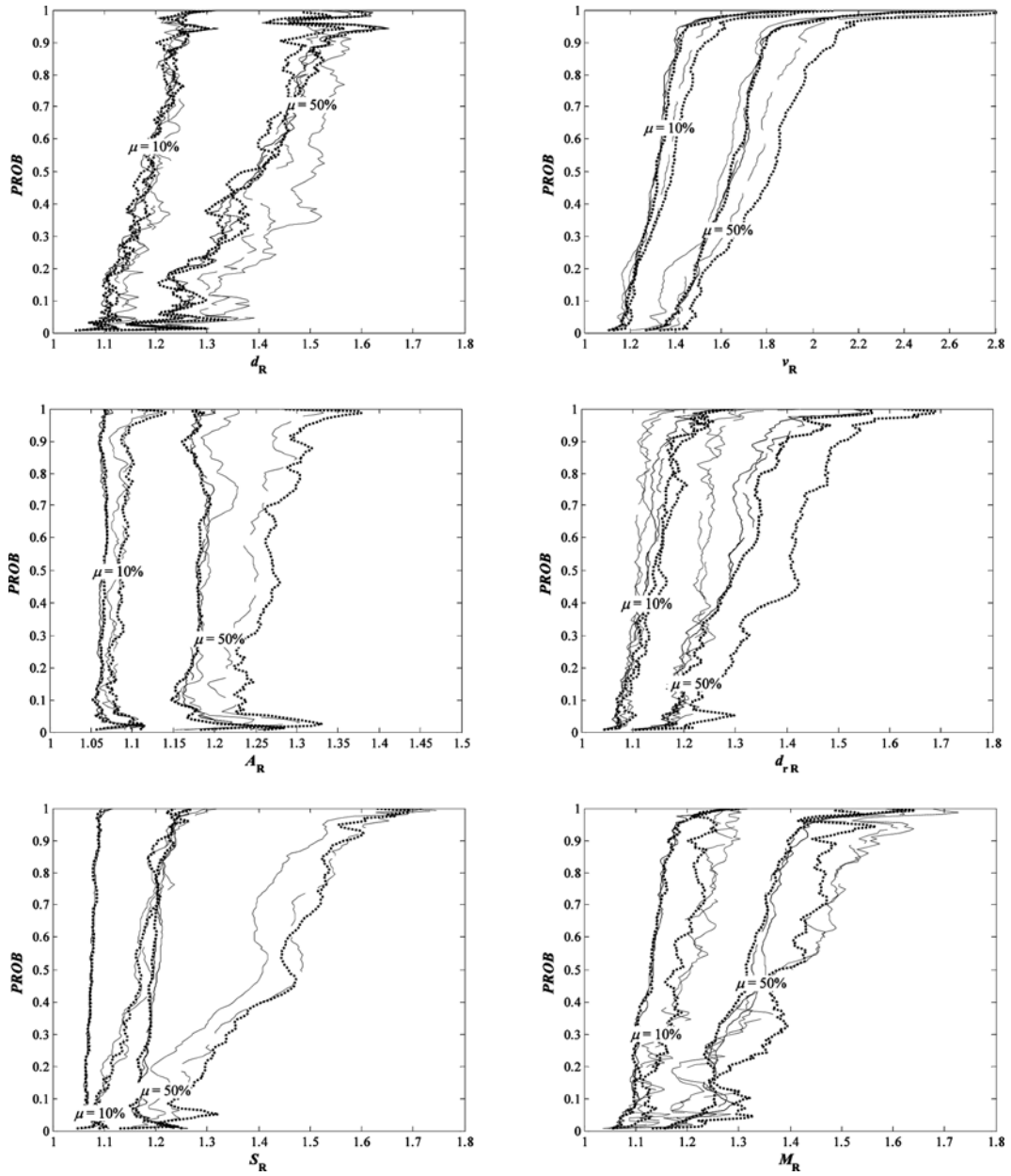

Fig. 7 Performance curves, under the FD set, for an H_∞^f-designed TMD with μ = 10% and μ = 50%, for the six MDOF models (- - - - Shear 1; - - - - Shear 2; —— Shear 3; - - - - Bending 1; - - - - Bending 2; —— Bending 3)

In analogy with the SDOF case, the following six response quantities are observed: the maximum peak relative displacement d; the square root of the total viscous energy dissipated by the structure during shaking, denoted as v because a weighted measure of RMS velocities; the maximum peak absolute acceleration A; the maximum peak inter-storey drift ratio d_r; the peak base shear force S; the peak base bending moment M.

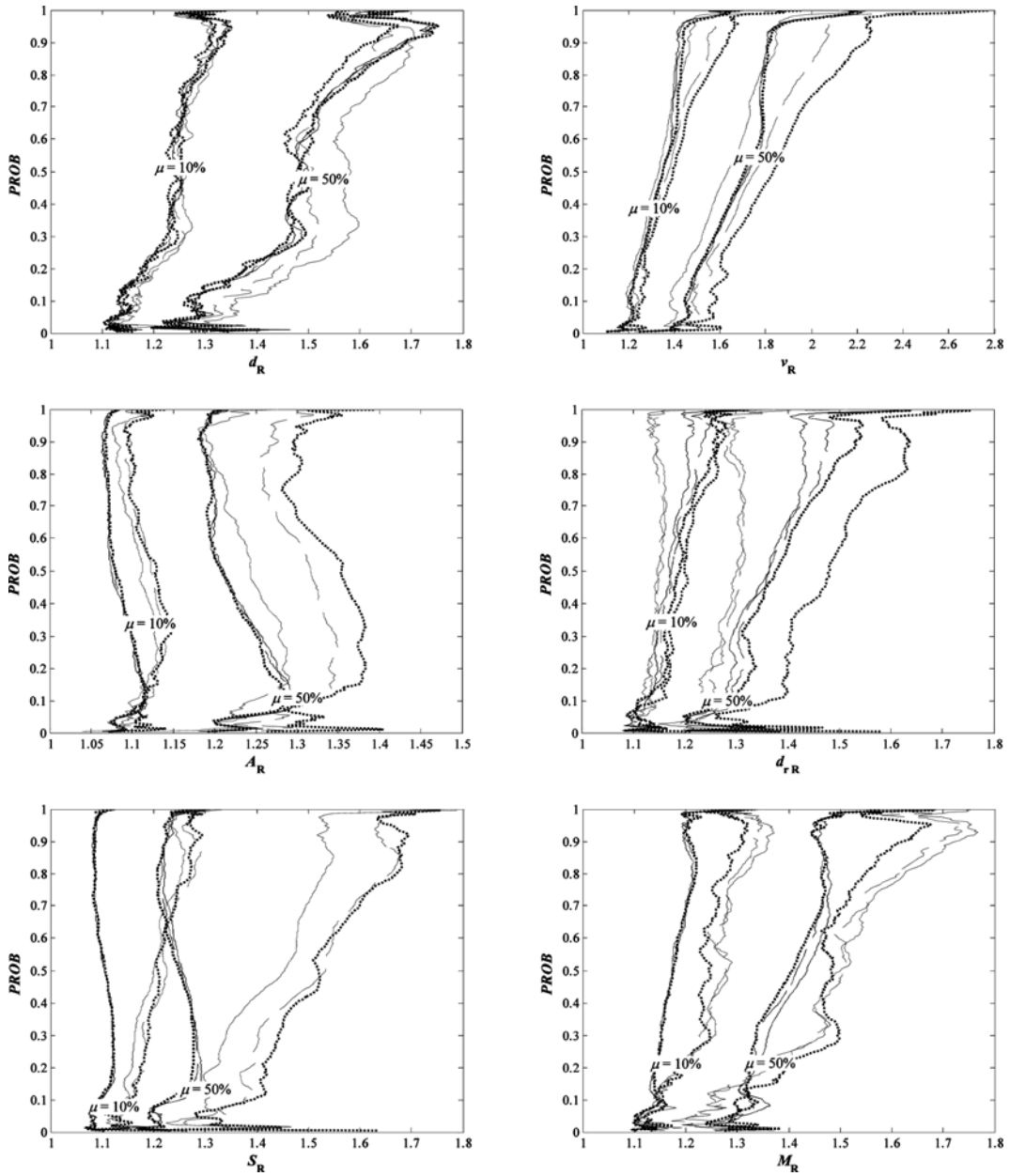

Fig. 8 Performance curves, under the NF set, for an H_∞^f-designed TMD with $\mu = 10\%$ and $\mu = 50\%$, for the six MDOF models (- - - - Shear 1; - - - - Shear 2; —— Shear 3; - - - - Bending 1; - - - - Bending 2; —— Bending 3)

The same five design criteria used for the SDOF case are here applied. For the first four criteria, the optimal parameters in Table 2, rigorously holding for SDOF systems only, are refined through numerically minimizing the respective norms of the MDOF TF from the base acceleration to the maximum inter-storey drift ratio. For the $D_{\max}$ criterion, parameters are the same as in Table 2.

For brevity's sake, results are shown for the H_∞^f criterion only, which has generally proven the best one (closely followed by H_2^f).

Reduction spectra are reported for the NF set and for the 95% percentile in Fig. 6, where the SDOF, the S_1 and the B_1 schemes are compared for μ = 10% and μ = 50%. TMD effectiveness is almost identical for the three schemes as long as T remains below a certain threshold, which considerably varies with the observed response, and is different for the S_1 and B_1 cases. For d_R, such threshold tends to infinity, i.e., the SDOF/MDOF equivalence substantially holds. But for v_R and, especially, for A_R, the contribution from the higher modes increasingly limits TMD effectiveness above respectively 1.0s and 0.5s, and more for the bending-type than for the shear-type buildings. For the remaining responses, d_{rR}, S_R, and M_R, the trend is someway intermediate between d_R and A_R. It can be concluded that, for sufficiently small periods, the results obtained for the SDOF system, particularly the performance curves in Fig. 5, are still valid for MDOF structures, whereas for larger periods TMD effectiveness can be reduced.

Keeping this in mind, the same averaging along the T axis already performed for the SDOF structure is here repeated for the six MDOF models in order to reconstruct the distribution curves, reported in Fig. 7 for the FD set and in Fig. 8 for the NF set.

Looking at Figs. 7 and 8 the following observations can be done.

- Apart from the d_R curves, which for the MDOF structures prove very similar to those drawn for the SDOF structure in Fig. 5, for all the other responses a general control loss is observed (particularly for v_R and A_R), but with a sharp distinction between the shear-type and the bending-type models. The TMD is still very effective for the shear-type models, yet with great differences among the three schemes (S_1 being the more effectively controlled). For building-type structures, control is heavily reduced, with negligible discrepancies among the three schemes. These differences can be explained by reconsidering Table 3. The best TMD performance corresponds to structural schemes in which the first modal mass is largely predominant, which also entails a larger TMD total mass ratio (the effective mass ratio being fixed).
- The "robust trend" already recognized in the SDOF performance curves (TMD effectiveness increasing with increasing percentiles) is generally maintained for MDOF structures.
- Forward directivity penalizes TMD effectiveness, but only slightly. Averaging over all curves and all percentiles, NF reduction is 1.032 times the FD reduction for μ = 10%, and 1.050 times for μ = 50%. Focusing on the 90-95% percentiles, the said values reduce to 1.026 and 1.041 respectively.
- TMD effectiveness increases with the mass ratio, but less than for the SDOF case. Averaging over all curves and all percentiles, TMD performance, when passing from μ = 10% to μ = 50%,

Table 4 Comparison of the five design methods

μ	H_2/H_∞^f	H_∞/H_∞^f	$D_{\max}/H_\infty^f$	H_2^f/H_∞^f
10%	0.996	0.991	0.973	0.996
50%	0.959	0.971	0.968	0.973

increases 1.17 and 1.19 times for, respectively, the FD set and the NF set. Focusing on the 90-95% range of percentiles, the said increments grow up to 1.21 and 1.22 respectively.

Previous results refer to the H^f_∞ design. Similar trends are observed for the other four optimization strategies. A concise comparison is given in Table 4, where the performance ratios, averaged over all response measures, all percentiles, and both sets of records, are reported for each method, normalized to those corresponding to the H^f_∞. The H^f_∞ method clearly appears the most effective, followed by the H^f_2 method.

5. Robustness of TMDs against detuning

TMDs are generally regarded to be scarcely robust against frequency "detuning", which can arise when the structural frequencies change due to stiffness or mass variations, or when the structure undergoes inelastic behaviour. Keeping to the assumption of structural linearity, the issue is here simplistically faced by means of Monte Carlo simulations, assuming that the fundamental structural period be a stochastic variable with a predefined probability distribution, namely a lognormal distribution having log-mean equal to the (nominal) period T and log-standard deviation equal to $0.2T$.

The spectral analysis is conducted in exactly the same manner as for the nominal case, except that for each T and for each record the analysis is run not only once but $N = 100$ times, each time randomly extracting the fundamental period from the lognormal distribution centred on T, while keeping constant the TMD parameters and the structural modal masses, modeshapes and damping ratios.

For brevity's sake, results are reported only for the design criteria showing the best performance, which are the H^f_2 for the SDOF case and the H^f_∞ for the MDOF cases.

In Fig. 9, which is the robust counterpart of Fig. 6, two differences with respect to the nominal case are noticeable: (a) robust spectral peaks are smoother since for each "nominal period" in the abscissa the analysis is repeated varying the "real period" according to the lognormal distribution; this makes representation clearer but above all makes it unlikely for the structure to miss the tuning to significant ground motion frequencies; (b) robust reduction spectra are only slightly lower than nominal ones.

Finally, Fig. 10 is the robust counterpart of Figs. 5, 7 and 8, although limited, for brevity, to d_R and A_R, and to the NF set. The variability of the structural period shows a negligible influence on d_R, and a small one on A_R, with the shape of the curves substantially unaltered. Not reported for brevity, FD set would show similar trends. Dividing point-by-point the nominal performance curves by the robust performance curves, and averaging over the structural schemes and the responses, the following values are obtained: for the FD set, 1.011 for $\mu = 10\%$ and 1.003 for $\mu = 50\%$; for the NF set, 1.017 for $\mu = 10\%$ and 1.008 for $\mu = 50\%$. Focusing on the 90-95% percentiles, the foregoing values respectively become: 1.028, 1.021, 1.036, 1.030. Evidently, the robust performance is only slightly diminished with respect to the nominal one.

6. Case-study: a roof-garden TMD against NF ground motions

This section suggests one possible solution for achieving the large mass ratios which are required

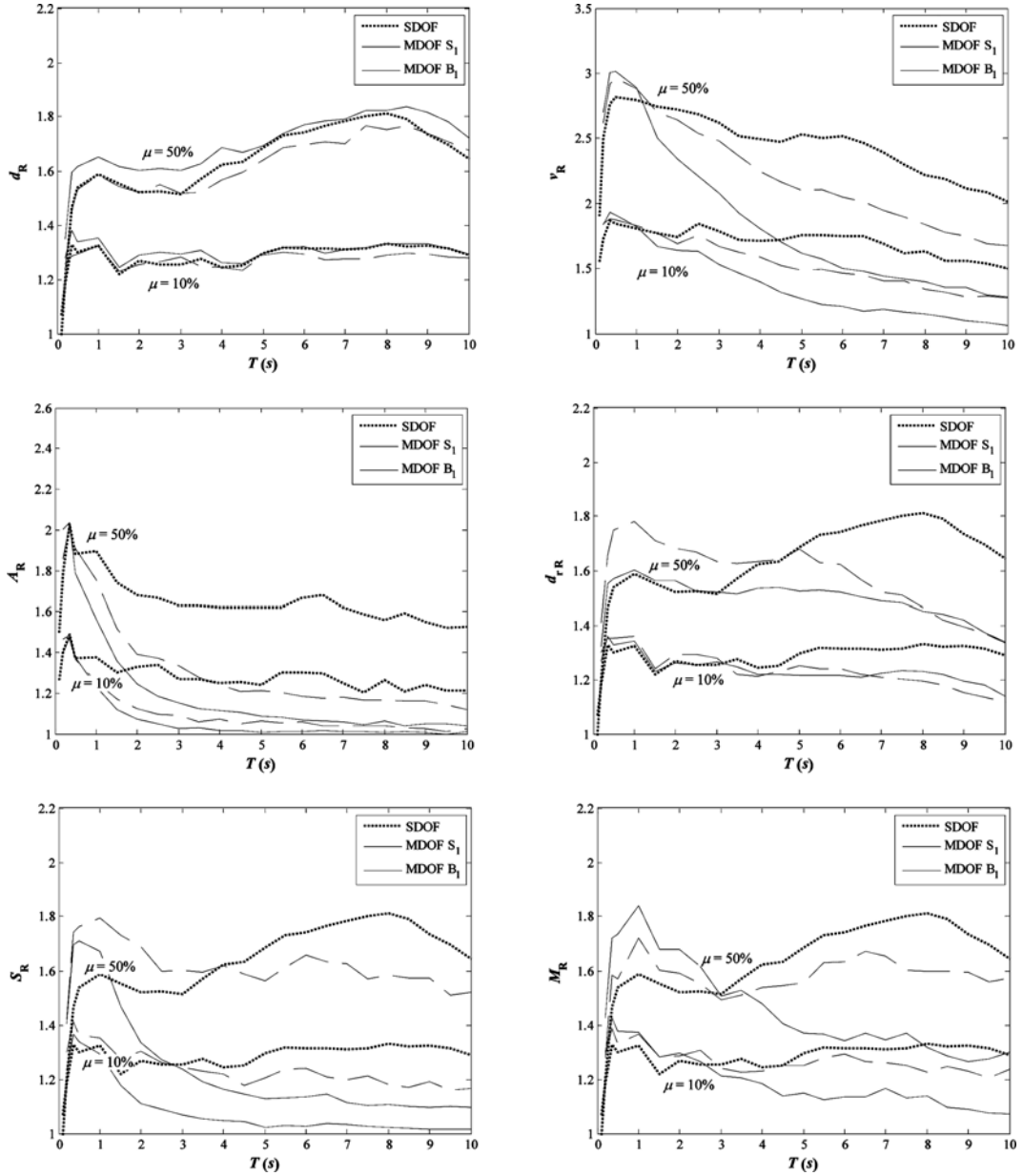

Fig. 9 95% percentile robust reduction spectra for the SDOF (H_2^f-designed TMD) and two MDOF (H_∞^f-designed TMD) systems, S_1 and B_1, under the NF set (μ = 10% or μ = 50%)

for a TMD to effectively control NF ground motions.

The example is the roof-garden TMD (RGTMD), proposed by the author to reduce the seismic response of a multi-storey building structure recently constructed in Siena, one of the most beautiful medieval towns in Central Italy (Matta and De Stefano 2009). The building is the D Unit of the Portasiena Linear Building complex, a polyfunctional commercial centre on which roof-gardens of the "intensive" kind were prescribed for architectural reasons. A rendering view of the complex and

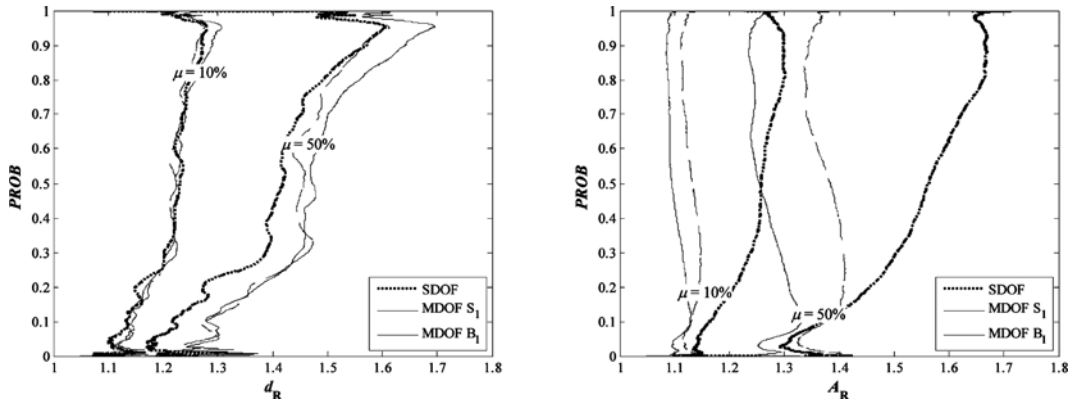

Fig. 10 Robust performance curves for the SDOF (H_2^f-designed TMD) and two MDOF (H_∞^f-designed TMD) systems, S_1 and B_1, under the NF set ($\mu = 10\%$ or $\mu = 50\%$)

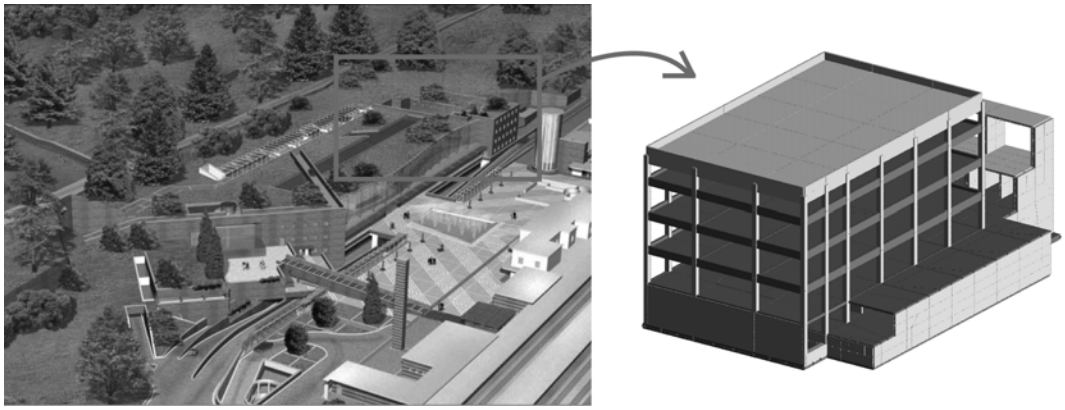

Fig. 11 Simulation of a roof-garden TMD in Portasiena Linear Building. Left: architectural rendering of the complex. Right: FEM model of the D unit

an axonometric projection of the full 3D FEM model for the D Unit are given in Fig. 11.

Involved in the structural design of the complex, the author explored the idea of turning the additional mass of the roof-garden into a passive TMD, with the purpose of combining environmental and seismic protection into a single device. This is achieved by adding a new floor atop the building, connected to the original top storey through a properly dimensioned system of bearings and dashpots, and filled with the planted soil.

A thorough description of the main structure and of three possible technological implementations of the RGTMD is given in (Matta and De Stefano 2009), where a classically H_∞-designed absorber was tested under 7 site-specific spectrum-compatible records. Like in that study, the main structure is here schematized as a planar 6DOF model with 5% damping in every mode. The three lower modes have natural frequencies 2.35 Hz, 9.29 Hz and 18.9 Hz and modal mass ratios 57.9%, 25.4% and 9.3%. The overall mass of the RGTMD (equal to 1270 kg/m^2) is 17.1% of the total mass of the building, corresponding to an "effective mass ratio" $\mu = 76.3\%$. Instead of the classical H_∞ design, the H_∞^f method is here applied by numerically minimizing the peak modulus of the Kanai-Tajimi filtered TF from the ground acceleration to the maximum interstorey drift ratio, resulting in the

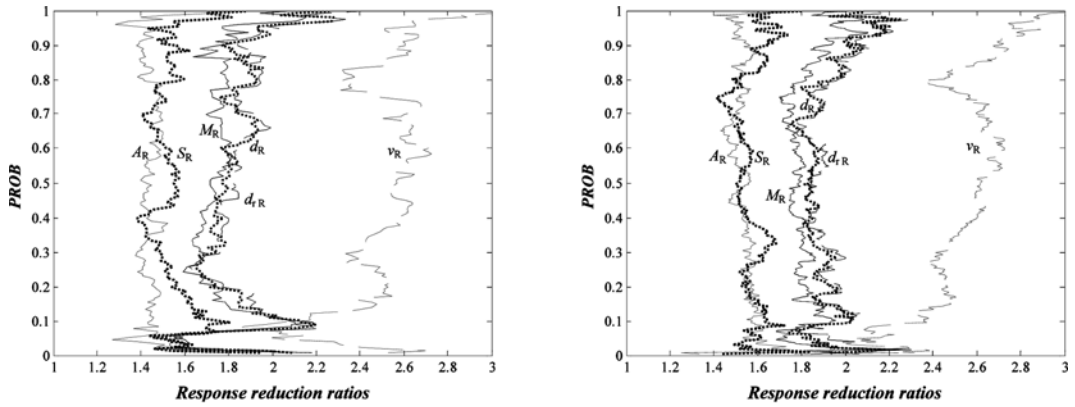

Fig. 12 Performance curves for the H_∞^f-designed RGTMD on Portasiena Linear Building, under the FD set (left) and the NF set (right) (- - - - d_R; - - - - v_R; —— A_R; - - - - $d_{r\,R}$; - - - - S_R; —— M_R)

optimal parameters $r = 0.528$ and $\zeta_t = 0.439$.

With and without the TMD atop, the structure is simulated under both the FD set and the NF set of records. The very satisfactory performance of the roof-garden TMD is shown by the performance curves in Fig. 12. By virtue of its large effective mass ratio, the RGTMD can significantly reduce all the observed responses, and more significantly those governed by the fundamental mode ($d_{r\,R}$, d_R and M_R) than those influenced by higher modes (A_R and S_R). Also, the performance against pulse-like records with forward-directivity effects (FD set) is only slightly inferior to that against the entire ensemble of near-fault earthquakes (NF set). Furthermore, not shown in the figures, the 95% percentile peak displacement of the TMD relative to the top storey is limited to 10.1 cm and 9.4 cm for, respectively, the FD set and the NF set; these values are perfectly compatible with a variety of constructive solutions for the bearing system of the RGTMD, including some simple and cost-effective rubber bearing arrangement as the one detailed in (Matta and De Stefano 2009).

7. Conclusions

In order to settle the existing controversy on the seismic efficacy of TMDs, this paper evaluates their performance against NF earthquake records, including ground motions with FD effects, critical because of their impulsive features. Based on the analysis of a large ensemble of natural records, percentile response reduction spectra and performance curves are introduced as the ideal tool to depict effectiveness and robustness of TMDs for seismic applications. The comparison of different design criteria (including two new variants), structural schemes, output measures, mass ratios and earthquake sets ensures some degree of generality to the results, which can be summarized as follows:

- TMDs are effective seismo-protective devices, provided that sufficient mass ratios are deployed (and except for very "rigid" structures); their peculiar ability to mitigate dynamic amplification reflects in their effectiveness increasing with the severity of the seismic effects; their robustness against both structure-to-earthquake "tuning" (shown by the proposed statistical evaluation) and absorber-to-structure "detuning" (proven through Monte Carlo simulations), is a fundamental

property of TMDs which part of the literature seems to have not fully recognized, and certainly not quantified.

- Larger in RMS terms than in peak terms, TMD effectiveness, nearly constant with T for an SDOF structure, for MDOF structures diminishes with T beyond a certain threshold, due to the contribution of uncontrolled higher modes; but not in the same manner for all output measures (displacement is almost unaffected, acceleration is affected most); also, the shear-type scheme resents less from this effect, and is more easily controllable than the bending-type. In any case, for MDOF structures the "effective mass ratio" is sensibly greater than the "total mass ratio", so the achievement of the requested large effective mass ratios is not unfeasible in practical applications. In this sense, the roof-garden TMD recently proposed by the author appears a promising solution, capable to incorporate dynamic and environmental protection into one single large device.
- Among the five optimization criteria compared in this study, the newly proposed H_2^f and H_∞^f, which incorporate, in the input-output TF, a Kanai-Tajimi filter centred on the structural frequency, prove the most efficient; the $D_{\max}$ criterion is confirmed to be ineffective for most response measures but proves the most beneficial for acceleration reduction.
- The impulsive character of FD records reduces TMDs effectiveness by only few percents with respect to generic NF quakes, with similar spectral trends. On a statistical basis, no indication is recognized discouraging the use of TMDs against pulse-like earthquakes.

Results above are circumscribed to the assumption of linear structural behaviour, holding all through the present study. Extension to the non-linear domain is left for future work.

References

Abdullah, M.M., Hanif, J.H., Richardson, A. and Sobanjo, J. (2001), "Use of a shared tuned mass damper (STMD) to reduce vibration and pounding in adjacent structures", *Earthq. Eng. Struct. D*., **30**, 1185-1201.

Abe, M. (1996), "Tuned mass dampers for structures with bilinear hysteresis", *J. Eng. Mech*., **122**, 797-800.

Baker, J.W. and Cornell, C.A. (2008), "Vector-valued intensity measures for pulse-like near-fault ground motions", *Eng. Struct*., **30**, 1048-1057.

Bernal, D. (1996), "Influence of ground motion characteristic on the effectiveness of tuned mass dampers", *Proceedings of 11th World Conference Earthquake Engineering*, Acapulco, June.

Bray, J.D. and Rodriguez-Marek, A. (2004), "Characterization of forward-directivity ground motions in the near-fault region", *Soil Dyn. Earthq. Eng.*, **24**, 815-828.

Chen, G. and Wu, J. (2001), "Optimal placement of multiple tuned mass dampers for seismic structures", *J. Struct. Eng.-ASCE*, **127**(9), 1054-1062.

Chiou, B., Darragh, R., Gregor, N. and Silva, W. (2008), "NGA project strong-motion database", *Earthq. Spectra*, **24**(1), 319-341.

Clark, A.J. (1988), "Multiple passive tuned mass dampers for reducing earthquake induced building motion", *Proceedings of 9th World Conference Earthquake Engineering*, Tokyo, August.

Gupta, Y.P. and Chandrasekaran, A.R. (1969), "Absorber system for earthquake excitation", *Proceedings of 4th World Conference Earthquake Engineering*, Santiago, January.

Hoang, N., Fujino, Y. and Warnitchai, P. (2008), "Optimal tuned mass damper for seismic applications and practical design formulas", *Eng. Struct*., **30**, 707-715.

Homma, S., Maeda, J. and Hanada, N. (2009), "The damping efficiency of vortex-induced vibration by tuned-mass damper of a tower-supported steel stack", *Wind Struct.*, **12**(4), 333-347.

Huang, Y.N., Whittaker, A.S. and Luco, N. (2008), "Maximum spectral demands in the near-fault region", *Earthq. Spectra*, **24**(1), 319-341.

Jagadish, K.S., Prasad, B.K.R. and Rao, P.V. (1979), "The inelastic vibration absorber subjected to earthquake

ground motions", *Earthq. Eng. Struct. D.*, **7**, 317-326.
Jangid, R.S. (2004), "Response of SDOF system to non-stationary earthquake excitation", *Earthq. Eng. Struct. D.*, **33**, 1417-1428.
Jara, J.M. and Aguiniga, F. (1996), "Parametric study of a two degree of freedom system with resonant masses", *Proceedings of 11th World Conference Earthquake Engineering*, Acapulco, June.
Kaynia, A.M., Veneziano, D. and Biggs, J.M. (1981), "Seismic effectiveness of tuned mass dampers", *J. Struct. Eng.-ASCE*, **107**(8), 1465-1484.
Leung, A.Y.T., Zhang, H., Cheng, C.C. and Lee, Y.Y. (2008), "Particle swarm optimization of TMD by non-stationary base excitation during earthquake", *Earthq. Eng. Struct. D.*, **37**, 1223-1246.
Li, C. and Qu, W. (2006), "Optimum properties of multiple tuned mass dampers for reduction of translational and torsional response of structures subject to ground acceleration", *Eng. Struct.*, **28**, 472-494.
Lin, C.C., Ueng, J.M. and Huang, T.C. (1999), "Seismic response reduction of irregular buildings using passive tuned mass dampers", *Eng. Struct.*, **22**, 513-524.
Lin, C.C., Wang, J.F. and Ueng, J.M. (2001), "Vibration control identification of seismically excited m.d.o.f. structure-PTMD systems", *J. Sound Vib.*, **240**(1), 87-115.
Lukkunaprasit, P. and Wanitkorkul, A. (2001), "Inelastic buildings with tuned mass dampers under moderate ground motions from distant earthquakes", *Earthq. Eng. Struct. D.*, **30**(4), 537-551.
Marano, G.C., Greco, R. and Palombella, G. (2008), "Stochastic optimum design of linear tuned mass dampers for seismic protection of high towers", *Struct. Eng. Mech.*, **29**(6), 603-622.
Matta, E. and De Stefano, A. (2009), "Seismic performance of pendulum and translational roof-garden TMDs", *Mech. Syst. Signal Pr.*, **23**, 908-921.
Melkumyan, M. (1996), "Dynamic tests of 9-story R/C full-scale building with an additional isolated upper floor acting as a vibration damper", *Proceedings of 3rd European Conference Struct. Dyn.*, Florence.
Miyama, T. (1992), "Seismic response of multi-storey frames equipped with energy absorbing storey on its top", *Proceedings of 10th World Conference Earthquake Engineering*, Madrid, July.
Park, J. and Reed, D. (2001), "Analysis of uniformly and linearly distributed mass dampers under harmonic and earthquake excitation", *Eng. Struct.*, **23**, 802-814.
Pinkaew, T., Lukkunaprasit, P. and Chatupote, P. (2003), "Seismic effectiveness of tuned mass dampers for damage reduction of structures", *Eng. Struct.*, **25**, 39-46.
Pourzeynali, S. and Zarif, M. (2008), "Multi-objective optimization of seismically isolated high-rise building structures using genetic algorithms", *J. Sound Vib.*, **311**, 1141-1160.
Rana, R. and Soong, T.T. (1998), "Parametric study and simplified design of tuned mass dampers", *Eng. Struct.*, **20**(3), 193-204.
Sadek, F., Mohraz, B., Taylor, A.W. and Chung, R.M. (1997), "A method of estimating the parameters of tuned mass dampers for seismic applications", *Earthq. Eng. Struct. D.*, **26**, 617-635.
Sinha, R. and Igusa, T. (1995), "Response of primary-secondary systems to short duration, wide-band input", *J. Sound Vib.*, **185**(1), 119-137.
Sladek, J.R. and Klingner, R.E. (1983), "Effect of tuned mass dampers on seismic response", *J. Struct. Eng.-ASCE*, **109**(8), 2004-2009.
Somerville, P.G., Smith, N.F., Graves, R.W. and Abrahamson, N.A. (1997), "Modification of empirical strong ground motion attenuation relations to include the amplitude and duration effects of rupture directivity", *Seismol. Res. Lett.*, **68**(1), 199-222.
Soto-Brito, R. and Ruiz, S.E. (1999), "Influence of ground motion intensity on the effectiveness of tuned mass dampers", *Earthq. Eng. Struct. D.*, **28**, 1255-1271.
Taflanidis, A.A., Beck, J.L. and Angelides, D.C. (2007), "Robust reliability-based design of liquid column mass dampers under earthquake excitation using an analytical reliability approximation", *Eng. Struct.*, **29**, 3525-3537.
Taniguchi, T., Der Kiureghian, A. and Melkumyan, M. (2008), "Effect of tuned mass damper on displacement demand of base-isolated structures", *Eng. Struct.*, **30**, 3478-3488.
Tothong, P. and Cornell, C.A. (2007), "Probabilistic seismic demand analysis using advanced ground motion intensity measures, attenuation relationships, and near-fault effects", PEER Report 2006/11, University of California, Berkeley.

Tsai, H.C. (1995), "The effect of tuned-mass dampers on the seismic response of base-isolated structures", *Int. J. Solids Struct*., **32**, 1195-1210.
Ubertini, F. (2010), "Prevention of suspension bridge flutter using multiple tuned mass dampers", *Wind Struct.*, **13**(3), 235-256.
Villaverde, R. (1985), "Reduction in seismic response with heavily-damped vibration absorbers", *Earthq. Eng. Struct. D*., **13**, 33-42.
Villaverde, R. and Koyama, L.A. (1993), "Damped resonant appendages to increase inherent damping in buildings", *Earthq. Eng. Struct. D*., **22**, 491-507.
Wang, J.F. and Lin, C.C. (2005), "Seismic performance of multiple tuned mass dampers for soil-irregular building interaction systems", *Int. J. Solids Struct*., **42**, 5536-5554.
Warburton, G.B. (1982), "Optimum absorber parameters for various combinations of response and excitation parameters", *Earthq. Eng. Struct. D.*, **10**, 381-401.
Wirsching, P.H and Campbell, G.W. (1974), "Minimal structural response under random excitation using vibration absorber", *Earthq. Eng. Struct. D.*, **2**, 303-312.
Wong, K.K.F. (2008), "Seismic energy dissipation of inelastic structures with tuned mass dampers", *J. Eng. Mech.*, **134**(2), 163-172.
Wu, W.J. and Cai, C.S. (2009), "Comparison of deck-anchored damper and clipped tuned mass damper on cable vibration reduction", *Struct. Eng. Mech.*, **32**(6), 741-754.